Structural investigation of thermo-mechanically processed Ti-29Nb-9Ta-10Zr alloy using X-ray diffraction

C.-M. TĂBÎRCĂ, D. RADUCANU, T. GLORIANT[a], D.-M. GORDIN[a], V.-D. COJOCARU, I. CINCA[*], I. DAN[b], A. CAPRARESCU

Politehnica University of Bucharest, Spl. Independentei 313, 060042 Bucharest, Romania

[a]UMR CNRS 6226 Sciences Chimiques de Rennes/Chimie-Métallurgie, 20 avenue des Buttes de Coesmes, F-35043 Rennes Cedex, France

[b]SC R&D Consulting and Services, Maria Ghiculeasa 45, 023761 Bucharest, Romania

During the last decades many researches were focused on titanium alloys used in biomedical applications, due to their favourable combination of mechanical resistance with physical and chemical properties such as: low density, high mechanical resistance, excellent corrosion and good biocompatibility. In the present paper, a Ti-29Nb-9Ta-10Zr (wt.%) alloy was thermo-mechanical processed and analysed in order to investigate structural changes occurred during processing. The alloy was fabricated by vacuum arc induction melting in a levitation furnace, FIVES CELES type, starting from elemental components and further thermo-mechanical processed. The X-ray diffraction investigation was used in order to characterize obtained structures during thermo-mechanical processing, using a Philip PW 3710 diffractometer, in Bragg-Brentano θ-2θ geometry, with negligible instrumental broadening. Data concerning alloys component phases, average coherent crystallite size and micro-strain at crystalline lattice level was obtained.

(Received March 25, 2013; accepted July 11, 2013)

Keywords: Titanium alloy, Thermo-mechanical processing, X-ray diffraction

1. Introduction

During the last decades, many researches were focused on titanium alloys used in biomedical applications, due to their favourable combination of mechanical resistance with physical and chemical properties such as: low density, high mechanical resistance, excellent corrosion and good biocompability. The addition of non-toxic elements such as niobium (Nb), tantalum (Ta) and zirconium (Zr) acts on β-phase stability and also is a way to improve mechanical properties [1-5].

Complementary, thermo-mechanical processing is often applied on titanium alloys in order to obtain a desired combination of mechanical properties based on various complex structures [6-9].

In the case of β-Ti alloys used in medical applications, especially in osseous implantology, a low elastic modulus is desired. In order to decrease the elastic modulus, microstructures consisting in a mixture of both β-Ti and α″-Ti phases must be obtained, due to the fact that α″-Ti phase exhibits a lower elastic modulus in comparison with parent β-Ti phase [10-15].

In this paper a Ti-29Nb-9Ta-10Zr (wt.%)β-Ti alloy was thermo-mechanical processed in different structural states, by homogenization, heavy cold-rolling, controlled recovery by recrystallization and annealing and investigated by X-ray diffraction, in order to determine formed structural phases and their associate parameters (crystalline lattice parameters; coherent crystallite size; micro-strain at crystalline lattice level).

2. Experimental

The investigated alloy has been produced using a vacuum arc induction melting in levitation furnace FIVES CELES with nominal power 25kW and melting capacity 30 cm^2, starting from high purity elemental components. Resulted chemical composition, in wt. %, was: 52%Ti; 29 Nb; 9Ta; 10Zr.

The thermo-mechanical processing route applied on Ti-29Nb-9Ta-10Zr alloy is presented in Fig. 1.

From as-cast alloy samples were cutted in order to process them by cold-rolling. Prior to first cold-rolling the samples were subjected to a homogenization heat treatment (structural state 1) in order to obtain an internal structure without major casting defects, such as segregation volumes. Heat treatment parameters were: homogenisation temperature: 950^0 C; treatment duration: 360 min, heating medium: high vacuum; cooling medium: furnace.

After homogenization treatment a cold-deformation process (structural state 2) was applied in order to refine internal microstructure. Cold-rolling deformation was used as deformation procedure, using a Mario di Mario LQR120AS laboratory roll-milling machine. Total

thickness reduction applied during cold-rolling was about 90%.

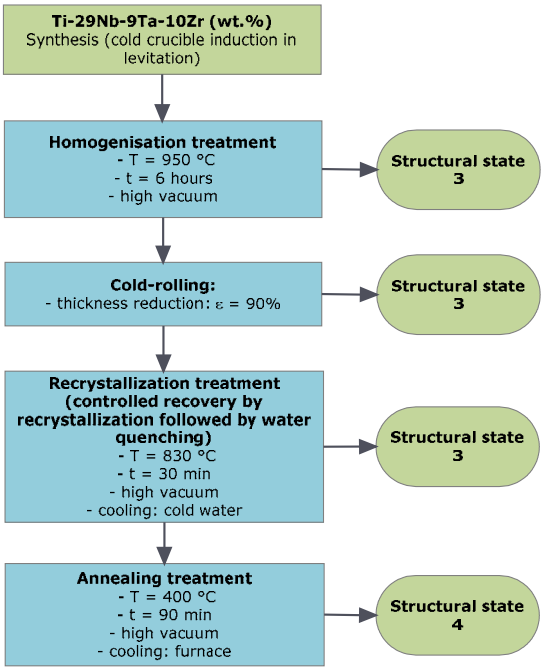

Fig.1. Schematic representation of thermo-mechanical processing route applied to Ti-29Nb-9Ta-10Zr alloy.

After cold-rolling a second heat treatment (structural state 3) was applied (controlled recovery by recrystallization, followed by water quenching) in order to remove unwanted cold-deformation effects, such as strain hardening, and to obtain a bimodal structure consisting of β-Ti and α″-Ti phases. The main heat treatment parameters were: recrystallization temperature: 830^0 C; recrystallization duration: 30 min, treatment medium: high vacuum; cooling medium: water.

A final annealing heat treatment (structural state 4) was applied with the aim to reduce internal micro-strain of both β-Ti phase and α″-Ti phases. Annealing heat treatment parameters were: annealing temperature: 400^0 C; annealing duration: 90 min, treatment medium: high vacuum; cooling medium: furnace.

All heat treatments were performed using a GERO SR 100X500/12 – high temperature furnace.

The XRD characterization was performed on all structural states, using a Philip PW 3710 diffractometer, in Bragg-Brentano θ-2θ geometry, using Cu Kα radiation (λ = 0.15406 nm). Prior to XRD measurements, upon all samples a metallographic polishing procedure was applied, in order to obtain flat surfaces, mirror polished, without any surface contamination.

All recorded XRD spectra were simulated and fitted. The XRD spectra simulation was performed using MAUD v2.33 software package, in order to calculate phases crystalline lattice parameters. The fitting procedure was performed using PeakFit v4.12 software package, in order to determine for each peak the position, intensity and peak broadening - FWHM (*Full Width at Half Maximum*). A pseudo-Voigt diffraction line profile was used in fitting procedure.

3. Results and discussion

3.1. Component phases

In the case of β titanium alloys the parent β-Ti phase can be transformed in hexagonal martensite (α′) or orthorhombic martensite (α″). Orthorhombic α″ martensite can be formed by transformation of the parent β phase during recrystallization or by *stress-induced transformation* [14]. The presence of α”- phase in the β-Ti alloys has a good influence on the mechanical properties, especially on elastic modulus, decreasing it’s value.

All structural states (1 to 4) were investigated using XRD diffraction. Recorded XRD spectra are presented in Fig. 2 – 5. As observed in Fig. 2, in the case of homogenized state (structural state 1) the microstructure consists of a single β-Ti phase. The β-Ti phase was indexed in body centered cubic system – *Im-3m*. Observed β-Ti diffraction peaks were as follows: (110), (200) and (211). In the case of 90% cold-rolled state (structural state 2) the microstructure consists of a mixture of β-Ti and α″-Ti phases, the α″-Ti phase being induced by *stress-induced transformation*. The α″-Ti phase was indexed in orthorhombic system - *Cmcm*.

Major diffraction peaks observed in the case of α″-Ti phase were as follows: (020), (111), (002), (022), (002), (220), (113) and (202).

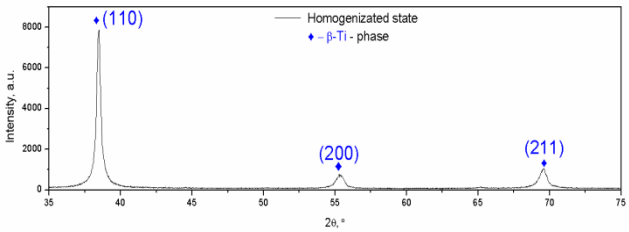

Fig. 2. XRD spectra of homogenized Ti-29Nb-9Ta-10Zr alloy (structural state 1).

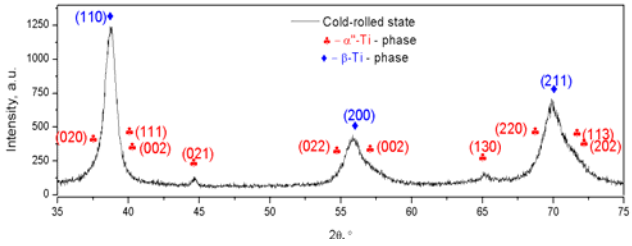

Fig. 3. XRD spectra of 90% cold-rolled Ti-29Nb-9Ta-10Zr alloy (structural state 2).

Both, β-Ti and α″-Ti phases are observed also in the case of recrystallized state (structural state 3) and annealed state (structural state 4), as observed in Fig. 4 and Fig. 5.

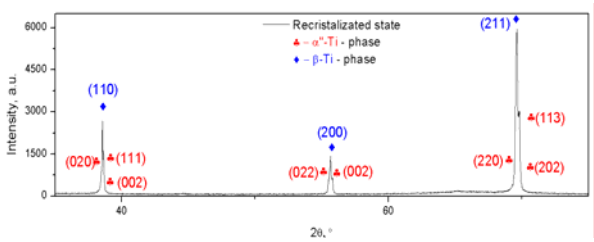

Fig. 4. XRD spectra of recrystallized Ti-29Nb-9Ta-10Zr alloy (structural state 3).

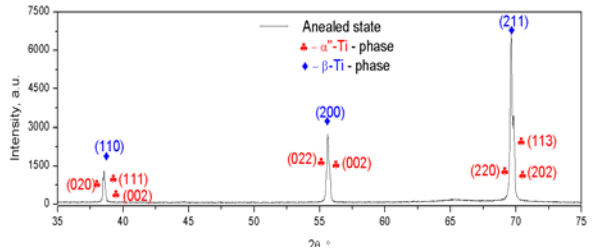

Fig. 5. XRD spectra of annealed Ti-29Nb-9Ta-10Zr alloy (structural state 4).

3.2 Lattice parameters

All XRD spectra's were fitted in order to deconvolute observed cumulative diffraction peaks and to obtain for each constitutive peak it's position, intensity and broadening.

Fig. 6 shows detailed zooms of cumulative diffraction peaks corresponding to 2θ = (30 - 40)° and 2θ = (60 - 70)° scattering angles, in the case of homogenized state (structural state 1). As observed, in both cases, only peaks of β-Ti phase are noticed.

In the case of 90% cold-rolled state (structural state 2), as observed in Fig. 7, in 2θ = (30 - 40)° scattering domain the following peaks sequence is observed: α″(020) – β(110) – α″(111) – α″(002). In the case of 2θ = (60 - 70)° scattering domain the observed peaks sequence is as follow: α″(220) – β(211) – α″(113) – α″(202).

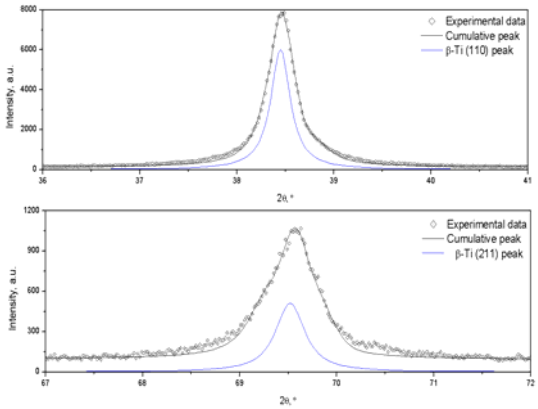

Fig. 6. Detailed zoom of (110) and (211) β phase diffraction lines corresponding to homogenized Ti-29Nb-9Ta-10Zr alloy (structural state 1).

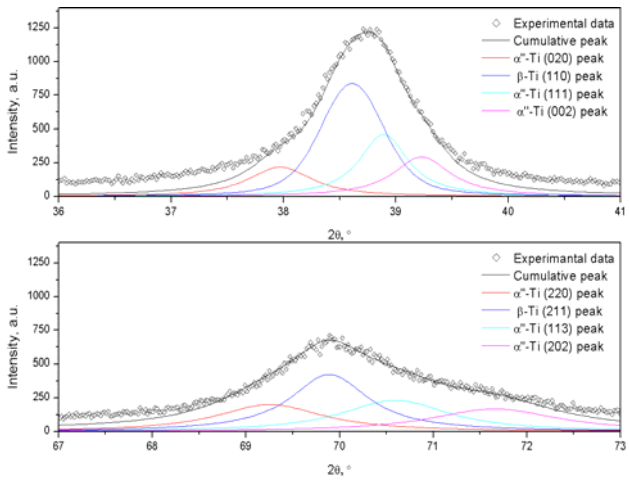

Fig. 7. Detailed zoom of (110) and (211) β phase diffraction lines corresponding to 90% cold-rolled Ti-29Nb-9Ta-10Zr alloy (structural state 2).

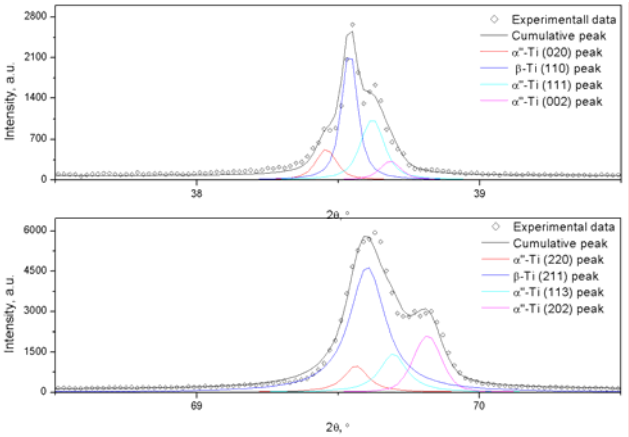

Fig. 8. Detailed zoom of (110) and (211) β phase diffraction lines corresponding to recrystallized Ti-29Nb-9Ta-10Zr alloy (structural state 3).

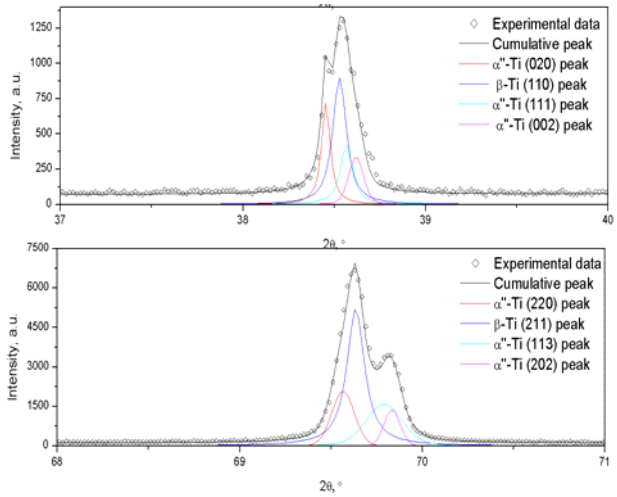

Fig. 9. Detailed zoom of (110) and (211) β phase diffraction lines corresponding to annealed Ti-29Nb-9Ta-10Zr alloy (structural state 4).

Same peaks sequences are observed also in the case of recrystallized state (structural state 3) and annealed state (structural state 4), as can be seen in Fig. 8 and Fig. 9.

For each diffraction peak it was obtained it's position, intensity and broadening.

Using obtained data concerning peak s position, computations were made in order to calculate crystalline lattice parameters in the case of both, β-Ti and α″-Ti phases. Obtained data were as it follows:

- Homogenized state (structural state 1):
  - β-Ti phase: a = 3,31 Å;
- 90% cold-rolled state (structural state 2):
  - β-Ti phase: a = 3,29Å;
  - α″-Ti phase: a = 3,21Å; b = 4,71Å; c = 4,61Å;
- Recrystallized state (structural state 3):
  - β-Ti phase: a = 3,31 Å;
  - α″-Ti phase: a = 3,30Å; b = 4,76 Å; c = 4,66Å;
- Annealed state (structural state 4):
  - β-Ti phase: a = 3,31 Å;
  - α″-Ti phase: a = 3,31Å; b = 4,75Å; c = 4,65Å;

Analysing the α″-Ti phase lattice parameters it is that in the case of 90% cold-rolled state the α″-Ti phase was obtained due to the stress-induced transformation, while in the case of recrystallized and annealed states was obtained due to the temperature-induced transformation.

3.3. Coherent crystallite-sizes and micro-strain at crystalline lattice level

Using obtained data concerning peaks broadening (FWHM - *Full Width at Half Maximum parameter*), further computations were made in order to calculate coherent grain-size domains and internal average micro-strain in the case of both, β-Ti and α″-Ti phases, for all investigated structural states.

In order to calculate coherent crystallite size and internal average micro-strain the Williamson-Hall equation [15] was used:

$$FWHM \cdot cos\theta = 0.9 \cdot \frac{\lambda}{D} + 4 \cdot \varepsilon \qquad (1)$$

where: FWHM parameter is the broadening of the diffraction peak measured as *Full Width at Half Maximum,* θ is the Bragg angle, λ is the wavelength of the X-ray radiation, ε is the average micro-strain and *D* the average dimension of crystallites (coherent grain-size).

Calculated coherent grain-size and internal average micro-strain values are presented in Table 1.

Table 1. Calculated coherent crystallite size and internal average micro-strain values in the case of homogenized, cold-rolled, recrystallized and annealed states.

Structural state	β-Ti - phase		α″-Ti - phase	
	ε [%]	D [nm]	ε [%]	D [nm]
Homogenized state	0.11	77.2	-	-
90% Cold-rolled state	0.32	23.9	1.32	57.4
Recrystallized state	0.18	33.1	0.11	22.4
Annealed state	0.06	36.5	0.08	23.3

It can be observed that in the case of homogenized state (structural state 1) the β-Ti phase show a grain-size close to 77.2 nm while the internal average micro-strain reaches a value close to 0.11%. A sharp decrease in coherent grain-size of β-Ti phase is noticed, in the case of cold-rolled state, to a value close to 23.9 nm, while the internal average micro-strain increase to a value close to 0.32%. Newly formed α″-Ti phase show a coherent grain-size close to 57.4 nm while its internal average micro-strain reaches 1.32%, in order to accommodate β→α″ stress-induced transformation.

The result of recrystallization and annealing treatments consists in small increments of coherent crystallite-size for both, β-Ti and α″-Ti phases, while the internal average micro-strain decreases dramatically.

4. Conclusions

The XRD investigations applied on Ti-29Nb-9Ta-10Zr (wt.%) alloy, thermo-mechanical processed, revealed that the phase components for all the studied samples, excepting homogenized state, consist of a mixture of β-Ti phase and α″-Ti phase.

The α″-Ti phase is obtained by stress-induced transformation in the case of 90% cold-rolled state while in the case of recrystallized and annealed states is obtained by temperature-induced transformation.

By applying an intense cold-rolling deformation processing a nanometrical microstructure, consisting in a mixture of β-Ti and α″-Ti phases is obtained; this nanometrical microstructure is retained also after recrystallization and annealing treatments.

Acknowledgment

This paper was supported by the UPB Project no. POSDRU/107/1.5/S/76903 - "Training of future researchers experts by Ph.D. scholarships" and also by a grant of the Romanian National Authority for Scientific Research, CCCDI – UEFISCDI, project number MNT-7-075/2013

References

[1] L. R. Ribeiro, R. C. Junior, F. F. Cardoso, R. B. F. Filho, L. G. Vaz, J. Mater. Sci. **20**, 1629 (2009).
[2] N. Tsuji, Y. Saito, S. H. Lee, Y. Minamino, Adv. Eng. Mater. **5**, 338 (2003).
[3] Y. Saito, H. Utsunomiya, N. Tsuji, T. Sakai, Acta Mater. **47**, 579 (1999).
[4] A. Azushima, R. Kopp, A. Korhonen, D. Y. Yang, F. Micari, G. D. Lahoti, P. Groche, J. Yanagimoto, N. Tsuji, A. Rosochowski, A. Yanagida, Compos. Manuf. Technol. **57**, 716 (2008).
[5] M. Niinomi, J. Mech. Behav. Biomed. Mater. **1**, 30 (2008).
[6] V. D. Cojocaru, D. Raducanu, D. M. Gordin, I. Cinca, J. Alloys Compd. **546**, 260 (2013).
[7] V. D. Cojocaru, D. Raducanu, T. Gloriant, I. Cinca, JOM-US. **64**, 572 (2012).
[8] D. Raducanu, V. D. Cojocaru, I. Cinca, I. Dan, Solid State Phenom. **188**, 59 (2012).
[9] D. Raducanu, V. D. Cojocaru, I. Cinca, I. Ichim, A. Schin, J. Optoelectron. Adv. Mater. **9**, 3346 (2007).
[10] S. A. Souza, R. B. Manicardia, P. L. Ferrandinib, C. R. M. Afonsoc, A. J. Ramirezc, R. Caram. **504**, 330 (2010).
[11] E. G. Obbard, Y. L. Hao, T. Akahori, R. J. Talling, M. Niinomi, D. Dye, R. Yang, Acta Mater. **58**, 3557 (2010).
[12] I. Costa, Mater. Corros. **58**, 329 (2007).
[13] T. Grosdidier, M. J. Philippe, Adv. Mater. Sci. Eng. **291**, 218 (2000).
[14] M. V. Popa, E. Vasilescu, P. Drob, V. D. Cojocaru, C. Vasilescu, Rev. Chim. (Bucharest, Rom.) **60**, 29 (2009).
[15] J. He, F. Zhou, G. Chang, E.J. Lavernia, J. Mat. Sci. **36**, 2955 (2001).

*Corresponding author: ion.cinca@mdef.pub.ro